

## EVAPORATION OF FREE WATER AND WATER BOUND WITH FOREST COMBUSTIBLES UNDER ISOTHERMAL CONDITIONS

A. M. Grishin, A. N. Golovanov, and  
S. V. Rusakov

UDC 533.6.011.6

*Evaporation of free moisture and bound moisture in the form of droplets lying on a rough surface, and also moisture bound with forest combustibles (FC) of coniferous trees is studied experimentally. Empirical formulas are obtained for the rate of evaporation of water droplets under isothermal conditions as a function of the diameter of the droplets and the wall roughness. The laws governing evaporation of bound moisture of FCs and combined evaporation of free and bound moisture have been studied.*

**Introduction.** It is assumed that water can interact with a material in several ways: chemically (at the molecular level), physicochemically (adsorption, osmotic, and capillary moisture), and physicom mechanically (droplet and film moisture) [1, 2]. Physicom mechanical moisture is also called free moisture, and chemical and physicochemical moisture is referred to as bound moisture. All types of moisture, except for chemically bound moisture, which possesses the highest energy of binding with a material, participate in the process of evaporation [2].

For mathematical description of the rate of evaporation of free water  $(\rho v)_w$  on a plane interface use is made of the Hertz–Knudsen law, which holds for evaporation from the free surface of the interface [3]:

$$(\rho v)_w = \frac{AM(p_s - p_e)}{\sqrt{2\pi MRT}}, \quad p_s = p_0 \exp\left(-\frac{L}{RT}\right). \quad (1)$$

The increased interest in evaporation of liquid droplets is due to the development of modern technologies of plasma-chemical deposition, deposition of thermoresistant coatings onto surfaces, and processes in the combustion chambers of heat-power plants and liquid-propellant rocket engines. Universal laws of evaporation of liquid spherical droplets have been derived [4, 5]:

$$D_\tau^2 = D_0^2 - k\tau, \quad k = \frac{8\lambda}{\rho_d c_p} \ln\left(\frac{L + c_p \Delta T}{L}\right), \quad \Delta T = T_g - T_d. \quad (2)$$

Relations were obtained for small and large droplets, respectively,

$$\frac{dr^2}{d\tau} = \text{const}, \quad (3)$$

$$\frac{dr}{d\tau} = \text{const} \quad (4)$$

which, as well as (2), are used in engineering calculations and for closing mathematical models of the processes of interaction of high-temperature heterogeneous flows with the surfaces in the combustion chambers and nozzles of reaction engines.

The process of evaporation of droplets for problems of jet cooling of a heated wall were studied in [6, 7] rather thoroughly. The radius of hemispherical droplets and droplets having the shape of a spheroid changes with time as

---

Tomsk State University, 36 Lenin Ave., Tomsk, 634050, Russia; email: fire@fire.tsu.tomsk.su. Translated from *Inzhenerno-Fizicheskii Zhurnal*, Vol. 76, No. 5, pp. 175–180, September–October, 2003. Original article submitted January 16, 2003; revision submitted April 30, 2003.

$$r = (r_d^{1.25} - 1.25A_1\tau)^{0.8}, \quad (5)$$

$$r = (r_d^{1.5} - 1.25A_2\tau)^{0.57}. \quad (6)$$

Formulas (5) and (6) hold under conditions of the absence of liquid sticking to the wall when the Leidenfrost phenomenon is observed [6]. In this case, at rather high temperature of the wall, a vapor layer, through which heat enters the droplet and is spent for evaporation, is formed between the wall and the droplet.

Data on evaporation of liquid droplets lying on the surface, where, along with forces of surface tension between the liquid and gas, there is surface tension between the liquid and the wall, are limited in number [8, 9]. However, precisely this formulation of the problem is topical, since it is related to cooling of surfaces, droplet condensation, different adsorption phenomena, etc.

Evaporation of bound water (drying of materials) is a complex multistage process which involves, except for desorption and adsorption of moisture, motion of water and vapor along the pores of the dried body and vapor flow in the boundary layer of the medium in the vicinity of the body [1, 2, 10]. Vast experimental data on drying of hygroscopical FCs — mosses, lichens, needle litter — is given in [11], where the effect of relative humidity  $\phi$ , temperature  $T$ , and initial humidity  $w_0$  on time of FC drying in the exsiccator is studied; this effect is determined as

$$\tau = \frac{2.3 [\log(w_0 - w_{eq}) - \log(w_\tau - w_{eq})]}{k}, \quad (7)$$

where  $\tau$  is the time, h. Formula (7) allows calculation of  $k$  for FC at a temperature of 293 K. Works devoted to investigation of the evaporation of free and bound water in the presence of liquid droplets and a porous body are absent.

**Aim of the Study and Experimental Technique.** The present work is aimed at experimental study of the evaporation of small droplets of water on a rough surface and water bound with FC. The necessity of these studies is related to the creation of a data base for a common mathematical model of forest fires within the framework of which an analog of formula (1) is used for mathematical description of evaporation of water droplets on the surface and in the pores of FC.

Evaporation of free water was studied on a transparent organic-glass backing of different roughness  $R_z$  which was placed in a drying stove, where the temperature was kept at a specified level  $T = (300 \pm 3)$  K. Water droplets were put on the backing by special needles and pipettes.

The roughness of the surface was determined by a profilometer-296 with an accuracy not higher than  $10^{-10}$  m; the roughness varied within the range  $R_z = (0.036-3.7) \cdot 10^{-6}$  m. A scale with a graduation of  $1 \cdot 10^{-3}$  m was fixed on the inner side of the backing in order to determine the initial diameter of the droplet  $D_0$ ; in this case,  $D_0 = (1-10) \cdot 10^{-3}$  m.

The mass of an individual droplet  $m_d$  was determined by continuous weighing of 8–10 droplets of the same size on an ADV-200 M analytical balance with an accuracy of  $10^{-4}$  g and subsequent division by a number of droplets in the sampling. The relative humidity of air in the drying stove  $\phi = p_e/p_s$  was monitored by an M-34 psychrometer and a VKF-43 microwave moisture meter; the atmospheric pressure  $p$  was controlled by a BAMM-1 aneroid barometer; the temperature of the surrounding air  $T$  was controlled by a laboratory mercury thermometer with a  $1^\circ\text{C}$  scale division. Total errors of the determination of parameters did not exceed  $\delta m \leq 2.1\%$ ,  $\delta T \leq 4\%$ ,  $\delta p \leq 3.7\%$ , and  $\delta \phi \leq 5.2\%$ . The confidence ranges of the measurement results were calculated proceeding from 3 to 5 experiments with a confidence probability of 0.95. Moreover, to confirm the validity and reliability of the measurement results, the mass of a droplet was found by the formula  $m_d = \rho_d V$ , where  $V$  is the droplet volume, which was calculated by the results of measurement of the height of the droplet  $h = O_1O$ , its radius  $r = O_1A_1$ , and the angle  $\Theta$  between the tangent and the liquid surface (Fig. 1). To obtain the droplet image on a monitor, from which  $h$ ,  $r$ , and  $\Theta$  were measured, a shadow method using the diaphragm was employed in order to eliminate interference phenomena in the schlieren [12].

A shape of the water droplet on the backing surface can approximately be taken to be a spherical segment whose volume was calculated by the formula [13]

$$V = \frac{1}{6} \pi h (h^2 + 3r^2). \quad (8)$$

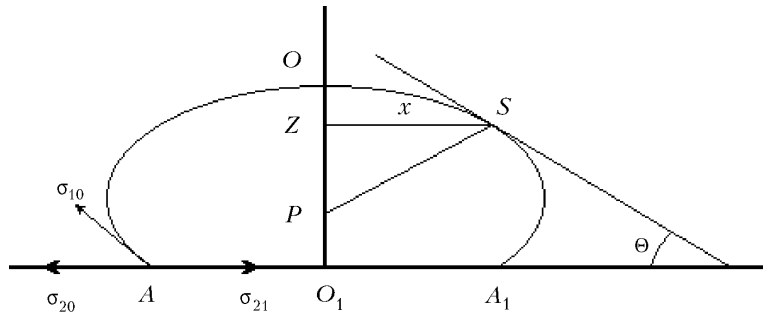


Fig. 1. Schematic representation of the droplet on the surface.



Fig. 2. Photograph of droplets on the schlieren at  $r = 4 \cdot 10^{-3}$  and  $20 \cdot 10^{-3}$  m.

For comparison purposes, Fig. 2 presents photographs of droplets on the schlieren for  $r = 4 \cdot 10^{-3}$  and  $20 \cdot 10^{-3}$  m which confirm the hemispherical shape of the droplets. This approximation is admissible for nonwetted and hydrophobic surfaces, since the droplet surface is rather complex and is described by the Adams–Bashforth formula [8]

$$2 + \beta \frac{z}{b} = \left( \frac{\beta V}{\pi x^2 b} + \frac{2 \sin \Theta}{x/b} \right), \quad (9)$$

where  $\beta = b^2 \rho_d g / \sigma$ ,  $x = ZS$ ,  $b = PO$ , and  $z = O_1Z$  (Fig. 1);  $\sigma$  is the coefficient of surface tension between the liquid and the gas. Results of the calculation of the volume of droplets by formulas (8) and (9) differ for droplets with  $D_0 = (1-10) \cdot 10^{-3}$  m by no more than 1%. The difference in the mass of droplets determined by the formula  $m_d = \rho_d V$  and by direct weighing was not more than 4%.

Moisture bound with FC was studied on typical elements of coniferous trees — needles of pine, cedar, and spruce. The specimens of the FC elements were placed in the drying stove at different temperatures of thermostating  $T = 303, 318, 325, 345, \text{ and } 369$  K. The parameters  $m$ ,  $\phi$ ,  $p$ ,  $T$ , and  $w = (m - m_0)/m_0$  were registered. In drying of forest combustibles, the dependence of the results of weighing on the density of specimen packing  $\rho_p$  and the volume of sampling  $V_{\text{sampl}}$  was found. Therefore, in each experiment the density of specimen packing remained constant and corresponded to a value close to the density of packing of needle litter under real conditions  $\rho_p \approx 11 \text{ kg/m}^3$ , and the value of the volume of sampling was determined from the condition  $V_{\text{sampl}} \ll 2\pi r_{\text{st}} H$ , where  $r_{\text{st}} = 0.12$  m and  $H = 0.24$  m.

**Results of the Investigation of Evaporation of Free Water.** Figure 3 shows some characteristics of the evaporation process as a function of time; here, curves 1, 2, and 3 are obtained for droplets with  $D_0 = 10 \cdot 10^{-3}$ ,  $6 \cdot 10^{-3}$ , and  $4 \cdot 10^{-3}$  m. The surface roughness was minimum ( $R_z = 0.036 \cdot 10^{-6}$  m). The solid lines in Fig. 3 are the bispline-approximation of experimental points. It is seen from the figure that the dimensionless height and mass of all droplets decrease linearly. Different laws governing evaporation of droplets (Figs. 3a and d) indicate the effect of surface roughness on the rate of liquid evaporation. Thus, forces of surface tension for spherical droplets have the same coefficient  $\sigma$ , whereas there exist three such coefficients for a droplet on the surface (see Fig. 1) [9]:  $\sigma_{21}$ ,  $\sigma_{20}$ , and  $\sigma_{10}$  — surface tension between the backing and the droplet, the backing and the air, and the droplet and the gas. Figure 4 illustrates the effect of the backing surface roughness on the decrease of a dimensionless mass of small droplets for  $D_0 = 4 \cdot 10^{-3}$  m, and curves 1, 2, and 3, respectively, refer to the results obtained for  $R_z = (0.036, 0.484, 3.7) \cdot 10^{-6}$  m. Evaporation of small droplets is more intense at a smaller roughness of the backing surface. The effect of surface roughness is less pronounced for large droplets and results of the measurements are within the confidence ranges. An increase of the backing surface due to its roughness leads to "sticking" of a larger number of molecules of the liquid to the backing,  $\sigma_{21}$  increases, and the rate of evaporation thus decreases due to a decrease in the number of molecules which have energy sufficient for overcoming the liquid-vapor interface. For large droplets, the effect of "sticking" of

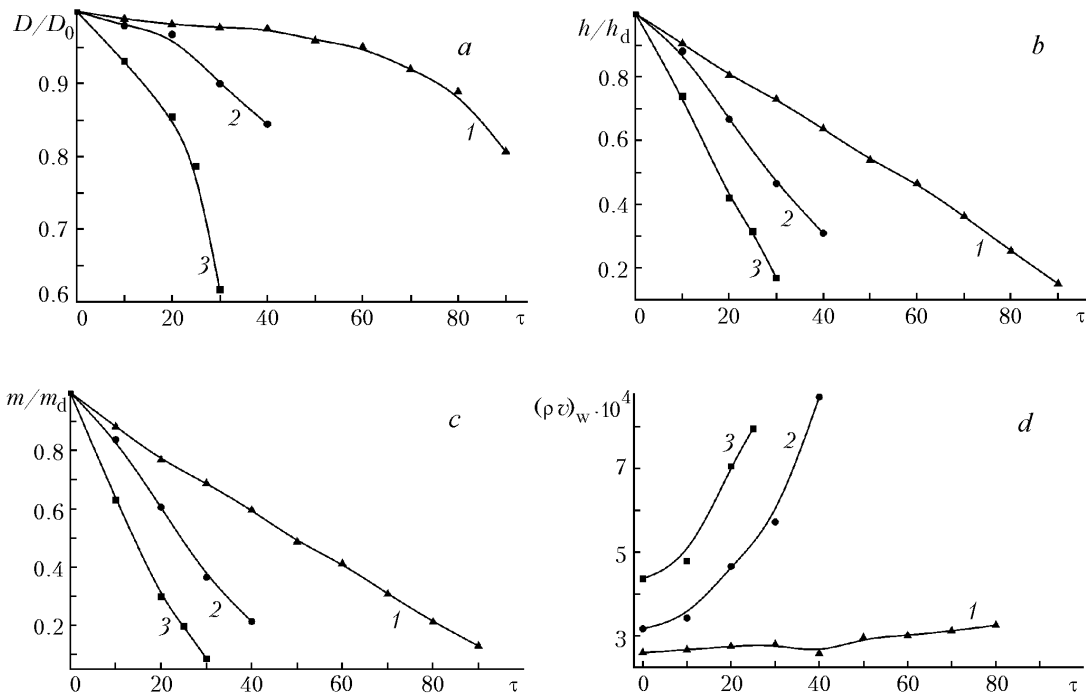


Fig. 3. Dependence of the diameter (a), height (b), mass (c), and evaporation rate (d) of the water droplet on a rough surface on time  $\rho(v)_w$ ,  $\text{kg}/(\text{m}^2 \cdot \text{sec})$ ;  $\tau$ , min.

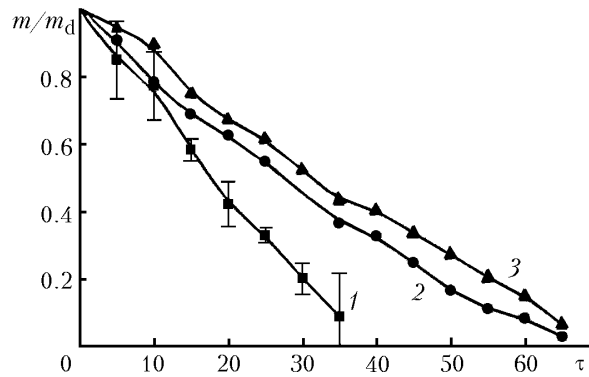


Fig. 4. Dependence of the decrease of a dimensionless mass of small water droplets on time at  $D_0 = 4 \cdot 10^{-3}$  m.  $\tau$ , min.

liquid due to roughness is smaller as a result of a relatively smaller surface and a larger height of a droplet  $h$ . For the same reason, at the initial instant the rate of evaporation of large droplets does not depend on time and forces of surface tension between the liquid and the wall impede a decrease of the initial diameter of the droplet  $D_0$ .

Evaporation of the droplets lying on the rough surface at  $D_0 = (1-10) \cdot 10^{-3}$  m,  $R_z = (0.036-3.7) \cdot 10^{-6}$  m, and  $T = (297-303)$  K obeys the law

$$\frac{m_\tau}{m_d} = 1 - 0.273 (1 - 1.08 \cdot 10^5 R_z) D_0^{-1.426} \tau, \quad (10)$$

obtained by approximation of the experimental results. The error of approximation of the empirical formula (10) is not higher than 8.4%.

The technique suggested for investigation of the process of evaporation of droplets lying on the backing surface allows rather accurate determination of the coefficient of surface tension between liquid and vapor  $\sigma_{10}$ . Making use of the dependence for additional pressure of vapor due to the curvature of the surface [14]  $p_v = 2\sigma_{10}/R_r$ , we find

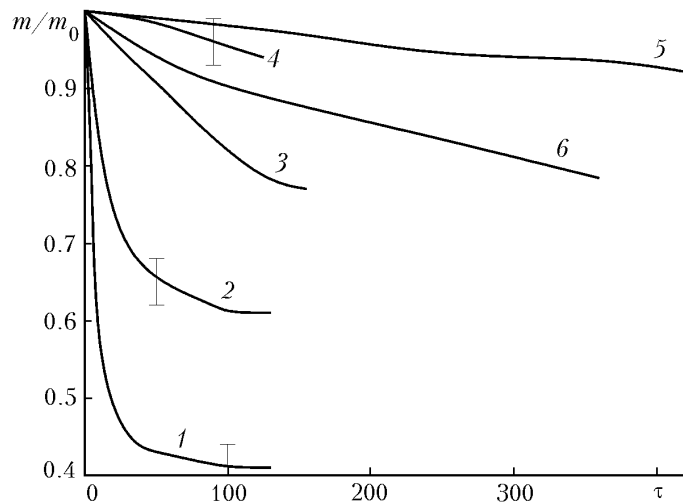


Fig. 5. Dependence of the decrease of a dimensionless mass of pine needles on time.  $\tau$ , min.

$$\sigma_{10} = \frac{R_r}{2} gh (\rho_d - \rho_v). \quad (11)$$

The value of the coefficient of surface tension for a water droplet at  $D_0 = 10 \cdot 10^{-3}$  m,  $T = 299$  K,  $\rho_v = 0.0243$  kg/m<sup>3</sup>, and  $R_r = 7.84 \cdot 10^{-3}$  m calculated by formula (10) is  $\sigma_{10} = 0.070$  N/m and differs from the tabulated value [15]  $\sigma = 0.072$  N/m by no more than 2%.

**Results of the Investigation of Evaporation of Bound Water.** Evaporation of water bound in FCs in their drying, which was realized at temperatures from 333 to 403 K, obeys the law [16]

$$\frac{dm}{d\tau} = - \frac{B(m - m_0) SM}{\sqrt{2\pi MRT}} \left[ p_0 \exp\left(-\frac{E_2}{RT}\right) - p_e \right]. \quad (12)$$

For high temperatures, the value of the pressure of saturated vapor is

$$p_s = p_0 \exp\left(-\frac{E_2}{RT}\right) \gg p_e, \quad (13)$$

and Eq. (12) is transformed as

$$\frac{dm}{d\tau} = - \frac{K_2(m - m_0)}{\sqrt{T}} \exp\left(-\frac{E_2}{RT}\right), \quad K_2 = \frac{Bp_0SM}{\sqrt{2\pi MR}}. \quad (14)$$

Figure 5 shows the typical dependences of the decrease in the mass of pine needles with time. Curves 1–5 are obtained at thermostating temperatures  $T = 369, 345, 325, 318,$  and  $303$  K. An exponential decrease of the mass of the specimens is traced at the beginning of the drying process for high temperatures (curves 1 and 2); then the needle mass reaches a certain stationary value. For low-temperature drying ( $T \leq 325$  K), portions associated with thermal inertia of the specimens are observed on the  $m/m_0$  curves. Curve 6 corresponds to the results of [11] obtained experimentally at  $\phi = 60\%$ ,  $T = 303$  K, and an initial humidity of the pine needles  $w_0 = 0.25$ . Curves 5 and 6 differ due to different values of  $\phi$  and  $w_0$  (in the present work they are 68% and 0.17, respectively). An increase in the initial humidity of air and decrease in the initial humidity of forest combustibles decelerate the process of desorption [11]. By the results of measurement of  $m/m_0$ , using Eq. (14) and the Freeman–Carroll method of straightening [17] we found the thermokinetic constants  $E_2/R$  and  $K_2$ .

Table 1 presents results of calculation of the thermokinetic constants obtained in different literature sources. The considerable scatter of the data is due to the different conditions of the experiments [18, 19] and the use of different techniques for processing the measurement results [20].

TABLE 1. Results of Calculation of the Thermokinetic Constants of Drying of Pine Needles

| Characteristics                      | Reference    |                  |                   |                  |
|--------------------------------------|--------------|------------------|-------------------|------------------|
|                                      | present work | [18]             | [19]              | [20]             |
| $T, K$                               | 303–369      | 369              | 333–403           | 273–293          |
| $E_2/R, K$                           | 4873         | 5247             | 5956              | 5185             |
| $K_2, K^{1/2} \cdot \text{sec}^{-1}$ | 13.5         | $1.5 \cdot 10^5$ | $6.03 \cdot 10^5$ | $2.8 \cdot 10^4$ |

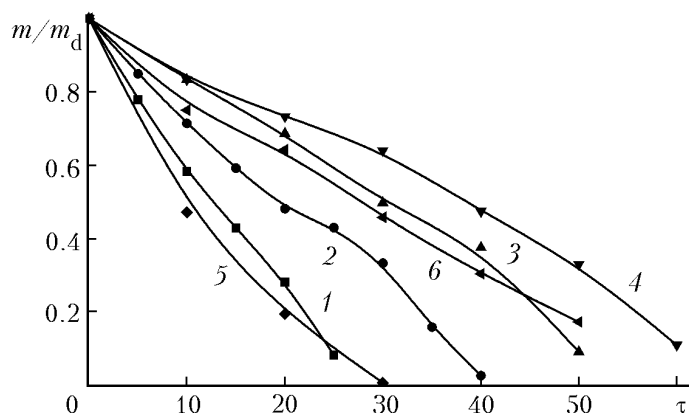


Fig. 6. Dependence of the decrease of a dimensionless mass of the droplet on wet and dry needles of spruce, cedar, and pine on time.  $\tau$ , min.

In closing, we note that of interest is the study of combined evaporation of free and bound water by an example of a water droplet lying on an individual needle. The conditions of this series of experiments are the following:  $T = 229 K$ ,  $p = 778 \text{ mm Hg}$ ,  $\phi = 0.82$ ,  $D_0 = 1 \cdot 10^{-3} \text{ m}$ ,  $w_1 = 1.84$ ,  $w_2 = 0.51$ ,  $w_3 = 0.35$ ,  $R_{z1} = 7.6 \cdot 10^{-6} \text{ m}$ ,  $R_{z2} = 4.4 \cdot 10^{-6}$ , and  $R_{z3} = 4.9 \cdot 10^{-6} \text{ m}$ , where the subscripts 1, 2, and 3 at water content and roughness refer to the needles of spruce, cedar, and pine.

Figure 6 presents the dependences of the decrease of mass of a droplet on wet and dry needles of spruce (curves 1 and 2), cedar (curves 3 and 4), and pine (curves 5 and 6). It is seen from Fig. 6 that dry needles do not take moisture from the droplet; therefore, curves 2, 4, and 6 lie higher than curves 1, 3, and 5. Weighing of dry needles after the experiments confirmed the absence of moisture exchange between dry needles and a droplet. The strongest difference in the rate of droplet evaporation is observed for pine needles, whose moisture content  $w$  is minimum and equals 0.35 (curves 5 and 6).

Needles of forest combustibles present a complex biological object represented by a porous body consisting of cells, moisture ducts, and air pores through which bound moisture is evaporated [21]. Visualization and microphotographs ( $\times 20$ ) show that air pores in dry needles are completely atrophied (see the photographs of needle cross sections in [21]); therefore there is no moisture exchange between a droplet and needles dried at  $T = 373 K$ . In wet needles, air pores are open, moisture from the droplet gets inside a needle through the surface, and the rate of evaporation of droplets on wet needles is higher than on dry needles.

## CONCLUSIONS

1. We studied the laws governing evaporation of free and bound water under isothermal conditions by an example of liquid droplets lying on the rough surface and in the FC layer.
2. An empirical formula is obtained for the rate of evaporation of small droplets with  $D_0 = (1-10) \cdot 10^{-3} \text{ m}$ . The laws governing evaporation of droplets lying on the surface greatly differ from those for evaporation of spherical droplets — the rate of the former is higher.
3. The surface roughness decreases the rate of evaporation of water droplets.

4. The formula for low-temperature drying of the FC layer is verified. It is shown that at a temperature  $T > 325$  K the partial pressure of water vapor can be disregarded in the formula for evaporation of bound water in forest combustibles.

## NOTATION

$(\rho v)_w$ , mass flow rate of evaporation of free water;  $A$ , coefficient of accommodation;  $M$ , molecular mass;  $L$ , heat of evaporation;  $R$ , universal gas constant;  $T$ , absolute temperature;  $T_g$  and  $T_d$ , temperatures of the gas and droplet;  $p_0$ , pressure in the liquid;  $D_0$  and  $D_\tau$ , initial and current diameters of the droplet;  $h_d$  and  $h_\tau$ , initial and current heights of the droplet;  $k$ , evaporation constant;  $\lambda$ , thermal conductivity of the gas;  $\rho_d$  and  $\rho_v$ , densities of the droplet and vapor;  $c_p$ , specific heat capacity of the droplet;  $r_d$  and  $r$ , initial and current radii of the droplet;  $R_r$ , curvature radius of the droplet;  $m_d$  and  $m_\tau$ , initial and current mass of the droplet;  $V$ , droplet volume;  $\sigma_{21}$ ,  $\sigma_{20}$ , and  $\sigma_{10}$ , surface tension between the backing and the droplet, the backing and the air, and the droplet and the gas;  $p_s$ , pressure of saturated vapor;  $p_e$ , partial pressure of water vapor;  $p_v$ , additional pressure of vapor;  $A_1$  and  $A_2$ , functions of thermophysical properties of liquid and vapor;  $\phi$ , relative humidity of air;  $p$ , atmospheric pressure;  $w$ , moisture content;  $w_0$ ,  $w_\tau$ , and  $w_{eq}$ , initial, current, and equilibrium humidity of forest combustibles;  $m$ , mass of needles;  $m_0$ , mass of dry needles;  $\rho_p$ , density of packing of specimens;  $V_{\text{sampl}}$ , volume of sampling;  $r_{\text{st}}$  and  $H$ , radius and height of the working chamber of the drying stove;  $S$ , effective surface area;  $B$ , compliance factor;  $E_2$ , effective heat of moisture evaporation;  $K_2$ , thermokinetic constant;  $R_z$ , size of surface roughness;  $g$ , free-fall acceleration;  $\tau$ , time. Indices: w, water; d, droplet;  $\tau$ , current value; g, gas; v, vapor; s, saturated; eq, equilibrium value; p, packing; sampl, sampling; st, stove; 0, initial value.

## REFERENCES

1. A. V. Luikov, *Heat and Mass Transfer: Handbook* [in Russian], Moscow (1978).
2. S. G. Romanovskii, *Processes of Thermal Treatment of Moist Materials* [in Russian], Moscow (1976).
3. B. V. Alekseev and A. M. Grishin, *Physical Gas Dynamics of Reacting Media* [in Russian], Moscow (1985).
4. F. A. Williams, *Combustion Theory* [Russian translation], Moscow (1971).
5. S. Lambarais and L. Combs, in: *Detonation and Two-Phase Flow* [Russian translation], Moscow (1966), pp. 270–309.
6. V. P. Isachenko and V. I. Kushnyrev, *Jet Cooling* [in Russian], Moscow (1984).
7. V. P. Isachenko, *Heat Transfer in Condensation* [in Russian], Moscow (1977).
8. M. J. Jaycock and G. D. Parfitt, *Chemistry of Phase Interfaces* [Russian translation], Moscow (1984).
9. Ya. E. Geguzin, *A Droplet* [in Russian], Moscow (1977).
10. A. V. Luikov, *The Theory of Drying* [in Russian], Moscow (1968).
11. V. I. Zhukovskaya, in: *Problems of Forest Pyrology* [in Russian], Krasnoyarsk (1970), pp. 105–140.
12. W. Hauf and U. Grigull, *Optical Methods in Heat Transfer* [Russian translation], Moscow (1973).
13. M. Ya. Vygodskii, *Handbook on Elementary Mathematics* [in Russian], Moscow (1976).
14. A. N. Matveev, *Molecular Physics* [in Russian], Moscow (1987).
15. N. B. Vargaftik, *Handbook on Thermophysical Properties of Liquids and Gases* [in Russian], Moscow (1972).
16. A. M. Grishin, *Mathematical Modeling of Forest Fires and New Methods of Fighting Them* [in Russian], Novosibirsk (1992).
17. Ya. A. Belikhmaier, N. M. Smolyanikova, and S. I. Smolyanikov, *Experimental Techniques: A Manual* [in Russian], Tomsk (1983).
18. A. M. Grishin, A. N. Golovanov, L. Yu. Kataeva, et al, *Fiz. Goreniya Vzryva*, No. 1, 65–76 (2001).
19. A. M. Grishin, V. E. Abaltusov, V. G. Zverev, et al., in: *Physics of Combustion and Methods of Its Investigation* [in Russian], Cheboksary (1981), pp. 129–139.
20. A. M. Grishin, A. Ya. Kuzin, and E. M. Alekseenko, *Inzh.-Fiz. Zh.*, **76**, No. 5, 170–174.
21. A. M. Grishin and A. N. Golovanov, *Inzh.-Fiz. Zh.*, **74**, No. 4, 53–57 (2001).